Research Square

Preprints are preliminary reports that have not undergone peer review.
They should not be considered conclusive, used to inform clinical practice,
or referenced by the media as validated information.

Interfacial Interactions and Tribological Behaviour of Metal-Oxide/2D-Material Contacts

Shwetank Yadav
University of Toronto
Taib Arif
University of Toronto
Guorui Wang
University of Toronto
Rana N.S. Sodhi
University of Toronto
Yu Hui Cheng
University of Toronto
Tobin Filleter
University of Toronto
Chandra Singh (chandraveer.singh@utoronto.ca)
University of Toronto

Research Article

Keywords: Nanotribology, MoS2, Graphene, Interfacial shear strength (ISS), DFT, Rutile (TiO2), Cupric oxide (CuO)

Posted Date: April 12th, 2021

DOI: https://doi.org/10.21203/rs.3.rs-373939/v1

License: This work is licensed under a Creative Commons Attribution 4.0 International License.
Read Full License

Abstract

This work combines experimental atomic force microscopy (AFM) and DFT simulations to study oxidized metal (oxidized copper & titanium) and 2D material (graphene & MoS2) interfaces. Combining AFM and DFT allowed identifying the interfacial interaction and established a correlation between tribological behavior, interfacial charge distribution, and variations in the potential energy profile with sliding along the metal/2D-materials interfaces. The TiO2 (rutile) and CuO (cupric oxide) metal oxides were mostly found to chemisorb along the interface with the 2D-materials. Both the metal-oxide counter-surfaces (TiO2 and CuO) exhibited higher friction force and adhesion on graphene than on MoS2. The CuO surface was inferred to be copper rich based on comparison with DFT simulations. The interfacial electronic charge distribution and relative energy change were identified to strongly influence sliding and adhesive behavior between oxidized-metal/2D-material contacts when considering only electronic effects in the DFT simulations. More homogenous interfacial charge distribution/sharing and lower surface energy variation, as found on the MoS2 surfaces, were identified to lower friction and adhesion. Non-electronic effects not captured by simulations were found to likely dominate interfacial shear strength measurements experimentally. Therefore, MoS2 should be used in interfacial applications involving TiO2 and copper rich CuO surfaces requiring lower adhesion and friction.

Introduction

Titanium and copper have been used extensively for decades to manufacture electrical and mechanical components. [1,2] At the macroscale, the tribological properties of metals can significantly improve when lubricated by lamellar-materials such as graphite and thick-MoS_2 primarily due to the formation of beneficial tribofilms. [2–5] The formation aids in the significant reduction of coefficient of friction (COF) and wear rate. [2,3,5] The structure of tribofilms can be complex, consisting of ultrathin-2D materials, unoxidized-metal and oxidized-metal species (e.g. CuO, TiO_2) when exposed to ambient conditions (e.g. air, water). [1] Identification of interfacial phenomenon for these individual species within tribofilms remains unknown mainly for macroscale studies since it is challenging to isolate them individually.[3] In-depth understanding of interfacial phenomena for 2D-materials and oxidized-metals has become vital as they are increasingly used together for designing nanoscale hybrid material systems.

Some of the applications of these nanoscale oxidized-metals/2D-material hybrid systems include advanced lubricants [2], electronics [6–8], and energy storage devices. [7,9] They exhibit superior properties including enhanced lubriciousness such as through a 50% reduction in coefficient of friction for copper/graphene vs. pure copper, hardness with an 80% increase for copper/graphene vs. pure copper, Young's modulus (e.g. 3-fold increase for copper/graphene vs. pure copper), wear resistance, thermal/electrical conductivity and fatigue resistance (5-6x enhanced fatigue resistance for copper/graphene vs. pure copper). [10–17] The improved properties are often dominated by the interfacial interaction between the metal/2D-material interface. [18,19] For instance, weakly interacting interfaces such as copper/graphene can minimize crack-formation/crack-propagation resulting in improved fatigue life

within nanoscale composite films. [16,20] Since emerging technologies such as flexible electronics are being designed using metal- and oxidized-metal/2D-materials, there is the need for studying and understanding the mechanisms in play at the interfaces which can affect processes such as delamination. Controlled experimental studies of oxidized-metal/2D-material interfaces remain a considerable gap in the current body of literature as existing atomic/nanoscale studies are primarily limited to atomistic simulations such as density functional theory (DFT).[21]

DFT studies are beneficial for gaining insight into atomic scale interfacial mechanisms by predicting the interaction between two surfaces, [21–24] the influence of changing interfacial energy profiles on sliding,[25] and identifying the correlation between interfacial charge distribution and friction/adhesion. [26,27] During sliding, interfacial interaction can vary depending on the relative position of two contacting surfaces and dictate adhesion at the atomic scale.[26] The interfacial energy corrugation acquired using DFT allows identifying the preferential sliding path with the lowest energy resistance for a given interface. [25] Wolloch et al. [26] recently reported a correlation between surface charge redistribution and surface energy corrugation with adhesion for contacting solid surfaces. Higher interfacial charge redistribution and greater change of interfacial energy were both reported to increase interfacial adhesion. [26] Interaction between pure metals and 2D-materials was predicted using DFT, where copper was reported to have a weaker physical interaction as compared with titanium, which exhibited a stronger chemical interaction with graphene. [21–24] In real applications, exposure of these metals to operational ambient conditions can quickly change the surface by forming oxide layers. Their influence on the interfacial interaction and tribological behavior with 2D materials remains unknown.

In this work, we custom-fabricate cantilevers to take an experimental atomic force microscope (AFM) based approach to compare the interfacial behavior of copper and titanium with ultrathin 2D-materials (graphene and MoS_2) at the nanoscale. In our study, by combining experimental AFM and DFT simulations, we first identify the surface chemistry of the metals (i.e. copper and titanium) and the interfacial interaction with ultrathin 2D-materials. Secondly, we study the effect of varying the interfacial interaction on sliding and adhesion. By comparing experimental AFM and DFT simulations, correlation is established between the tribological behavior, the interfacial electronic charge, and the changing interfacial energy profile along the metal/2D-material interfaces.

Results And Discussion

Characterization of copper and titanium counter-surfaces

Analytical high-resolution X-ray photoelectron spectroscopy (XPS) was used herein to characterize copper and titanium samples to understand the metal surface chemistry (Figure 1). It was found that both the metals had undergone surface oxidation. The titanium surface is composed primarily of TiO_2 (Figure 1a, b), where the Ti2p peak energy confirmed the TiO_2 to have a rutile structure.[28] Furthermore, traces of Ti metal, TiO and Ti_2O_3 compounds were detected from the subsurface (Figure 1b). The thickness of the

oxide was estimated by comparing the relative intensities of the Ti2p, Ti3p regions, where the difference in the mean free path due to the universal curve can be used to estimate the thickness of the overlayers (Supporting Information; Section S1). Herein the thickness of the titanium oxide layer was calculated to be ~1.1nm.

Analysis of the copper sample identified the presence of cupric oxide (CuO) as the outermost layer (Figure 1c). Due to the small chemical shifts observed between Cu and its oxides, the copper oxides were analyzed by a chemical depth profile approach using monotonic Ar^+ etching while analyzing the copper Auger peak. Mathematical integration of the area under the Auger peak allowed for Cu in its different oxidation states to be followed as a function of depth (Figure 1d and Supporting Information; Figure S1). It was found that a thin layer of CuO existed as the outermost layer followed by ~6 times thicker Cu_2O subsurface underneath (Figure 1d). The total thickness of the copper oxide layer is estimated to be ~3.3nm.[29,30] Oxidized copper and titanium beads were attached to tipless cantilevers to act as counter-surfaces (Figure 1e, f) for tribological testing and were studied against ultrathin-graphene or ultrathin-MoS_2 samples in the following section (Figure 1g).

Experimental study of metal-oxide/2D-material interface

Friction, interfacial shear strength (ISS), and adhesion on ultrathin-graphene (Figure 2a) and ultrathin-MoS_2 (Figure 2b) were measured against custom-fabricated CuO and TiO_2 counter-surfaces (Figure 1e-g) using AFM contact mode microscopy. Friction force microscopy (FFM) was performed as a function of normal load (F_N:0-2000 nN) while ensuring all the interfaces to remain in a wear-free regime (Figure 2). Friction results were repeatable for three separate datasets. On graphene, overall higher friction and adhesion for TiO_2/graphene than CuO/graphene was observed (Figure 2a & Table 1). ISS was measured by fitting the friction-normal load plot using the procedure proposed by Carpick et al. [31] (Supporting Information; Figure S2). Carpick et al. developed a parametrized approach based on Maugis-Dugdale model. [31] The procedure allows for understanding the range of surface forces at the contact, the contact and extract ISS by fitting the FFM data. The interfacial shear strength (ISS) was measured to be ~21.3 ± 6.8 MPa for CuO/graphene and ~83.4 ± 18.1 MPa for TiO_2/graphene interface (Table 1).

Similarly, MoS_2 samples (i.e. TiO_2/MoS_2 vs CuO/MoS_2) also exhibited an overall higher friction and adhesion when in contact with the TiO_2 counter-surface, with ISS measured to be 76.2 ± 17.3 MPa between TiO_2/MoS_2 interface (Figure 2b & Table 1). The more resistive sliding behavior on the TiO_2 counter-surface was accompanied by higher interfacial adhesion (Table 1). As for CuO counter-surface, there was a greater relative change in friction force as a function of normal load compared to other interfaces and ISS between CuO/MoS_2 was measured to be 13.8 ± 4.9 MPa (CuO/MoS_2). It the later section using DFT, it was observed that the interfacial behavior along MoS_2 is highly sensitive to any presence of exposed oxygen on the oxidized-copper counter-surface. Furthermore, comparison of graphene and MoS_2 using the same counter-surface (e.g. CuO/graphene vs CuO/MoS_2) shows lower adhesion and friction at low normal loads on MoS_2 than on graphene (Table 1) for both the counter-

surfaces, when the sliding behaviour is dominated by interfacial interaction. However, the CuO/MoS_2 has greater change in friction with normal load and exhibits higher friction during sliding at high loading regime. Adhesion on graphene was measured to be several folders higher using the same metal oxide counter-surface than that on MoS_2 (Table 1). To gain insight on the interfacial interaction/mechanism, in-depth DFT simulations were conducted to simulate sliding interfaces, and are presented in the subsequent section.

DFT simulations of metal-oxide/2D-material interface

In this section, the interfacial interaction between metal-oxide counter-surfaces (CuO and TiO_2) and 2D-materials (graphene and MoS_2) were investigated using DFT (Figure 3a,b). In the case of CuO counter-surface, two possible surface terminations (i.e. oxygen-rich and copper-rich) arise due to alternating layers of Cu and O atoms (Supporting Information; Figure S4). Additionally, the CuO counter-surface was also simulated with the less oxidized Cu_2O subsurface layer (i.e. Cu_2O + CuO) earlier identified in Figure 1. Unlike CuO, the TiO_2 structure has no such distinguishable layers, resulting in a single surface termination (Figure 3a). A TiO_2/bilayer-MoS_2 system was also investigated to gain insight into dthe effect of 2D material thickness on interfacial interaction (Table 1).

For all the material systems, the change in relative energy (with regards to initial step) was tracked as the metal-oxide counter-surfaces translated in incremental sliding steps (Δd) along the 2D-material basal plane. The interface was allowed to relax at each sliding step, in the direciton normal to each surface, and the change in relative energy (ΔE) was used to evaluate the ISS (τ), where $\tau = \Delta E / \Delta d$ (Supporting Information; Figure S3). In general, the sliding of metal-oxide counter-surfaces along the graphene basal plane was observed to have higher ISS than MoS_2 for the same metal-oxide (Tables 1 & S2). The metal-oxides had to overcome higher energy barriers along the graphene basal except for the CuO (O-surface) counter-surface, where sliding along MoS_2 basal plane was found to be more resistive than graphene (Supporting Information; Figure S3 & S4). The highest average ISS of all systems occured for CuO (Cu-surface) with graphene, while the lowest occured for the CuO (O-surface) with graphene (Supporting Information; Table S2).

Table 1: Comparison of theoretical DFT predictions and experimental measurements for oxidized-metal/2D-material interfaces. Max energy difference (ΔMax Energy) refers to the difference between relative energies of the least and most stable positions along sliding path. Adsorption distance is for the most stable (lowest energy) position along the path. Average ISS is reported with standard deviation. F_{POF} is the pull off force to measure adhesion between the interface. F_f is the friction force with 0nN normal load. ISS_{Exp} is the experimental interfacial shear strength measured from friction force. All experimental interfaces composed of ultrathin-2D materials (i.e. not mono/bilayer 2D material)

Counter-Surfaces & 2D-Material Interfaces		DFT Simulations		Experimental		
		ΔMax Energy [meV/ Å^2]	**ISS Average** [MPa]	**F_{POF}** [nN]	**F_f** [nN]	**ISS Exp** [MPa]
TiO_2	**graphene**	6.70	950 ± 780	959 ± 5	11.4 ± 0.3	83.4 ± 18.1
	MoS_2	3.49	300 ± 180	464 ± 12	9.5 ± 0.5	76.2 ± 17.3
	Bilayer- MoS_2	3.79	330 ± 190	-	-	-
Cu_2O + CuO (Cu-surface)	**graphene**	13.53	1540 ± 760	282 ± 17	4.1 ± 0.2	21.3 ± 6.8
	MoS_2	0.99	110 ± 80	41 ± 1	1.7 ± 0.3	13.8 ± 4.9

The interfacial adsorption distances (d_{ad}) between the oxidized-metal counter-surfaces and 2D-material basal planes were calculated to establish the interaction regimes (chemical or physical interaction) (Table 1). The interfacial adsorption distances (d_{ad}) were acquired for the lowest energy depicting the most stable configuration (Supporting Information; Table S1). Previous studies have denoted adsorption distance between 2.0 < d_{ad} < 2.5 Å as chemical interactions. [21] According to the above distance criteria, all of the systems display chemisorption behavioiur (Table 1) with the exception of the CuO-(O-surface)/graphene system (Supporting Information; Table S1). While the majority of interfaces are interacting chemically, the metal-oxide/2D-material interfaces exhibit varying ISS values suggesting additional interfacial mechanisms contributing to the ISS. Along the sliding path, larger electron density and bonding variations result in larger changes in local chemical environment as atoms pass through. These variations are tyically caused by increased electron localization for surface atoms, whereas a more uniform electron distribution is caused by a metal like spread out of the electron distribution. This is in agreement with the correlation that higher relative energy change results in higher ISS (Tables 1 & S2).

Figure 3 displays the electron localization function (ELF) graphs for a cross-section of the interfaces at their lowest energy step, giving a snapshot of the interfacial electronic distribution. For the TiO_2/graphene interfacial ELF (Figure 3a), it can be seen that there are regions of very low charge (red color) in between carbon atoms of the graphene sheet along the sliding interface. On the other hand, for MoS_2, there is a more even spreading of charge, with a yellow contour of charge always presents between S atoms of the MoS_2 sheet. Therefore the TiO_2 counter-surface atoms experience a less drastic change in the local environment, implying less energy variation and sliding resistance along the MoS_2 basal plane. ELF analysis for Cu_2O+CuO counter-surface along the graphene interface also illustrates electron concentration variation with clear regions of red along the sliding interface (Figure 3b). Along MoS_2 basal plane, no red regions and sharp change in interface charge were observed, resulting in lower ISS in comparison to graphene. This is consistent with literature, which reports that lowering the energy barrier results in lower friction when comparing graphene and MoS_2. [32] However unlike metal oxide counter-surfaces, Vaziriserehk et al[32] reports lower friction on graphene than on MoS_2 against SiO_2 tip. This highlights the significane of counter-surfaces on the interfacial energy landscape.

Overall, if the metal oxide surface termination has metal atoms (copper or titanium), then graphene will present higher ISS. However, if there is an oxygen termination, the MoS_2 will have higher ISS. The presence of an additional layer of 2D material, at least for the TiO_2/MoS_2 case, did not significantly alter the sliding behavior of the interface. This is likely affected by the fact that interlayer spacing for bulk solids of the 2D materials (~3 Å for MoS_2 [33] and 3.3 Å or higher for graphite [34]) is higher than the adsorption distances for the interfaces. The CuO surface with Cu_2O subsurface, implying less oxygen content as one moves away from the surface into the bulk, results in a reduction of ISS for both graphene and MoS_2 interfaces, with the latter seeing a much greater reduction.

Comparison of Experimental and Theoretical Trends

It should be noted that simulation results are only useful for obtaining qualitative relative trends between surfaces and their quantitative numerical predictions cannot be compared to experimentally measured values as complex real world surfaces are not well captured by the atomic scale DFT models. The DFT simulations are capturing nuclear and electronic interaction which can represent chemical bonding and van der Waals attraction. The insight provided by DFT is that it can isolate these factors and their contribution to friction behaviour (qualitatively), among a number of other factors affecting total friction force measurements.

A comparison between experimental and DFT simulation reveals similar general trends. Experimentally graphene was found to consistently exhibit higher friction and adhesion as compared to MoS_2 against both TiO_2 and CuO counter-surfaces. Higher friction trend on graphene as compared to MoS_2 was also observed using DFT simulations. In the case of CuO counter-surface, experimentally, it is difficult to precisely characterize and control the termination of a surface layer, as was achieved in simulations (O-surface vs Cu-surface). Hence, experiments reported only a single CuO system for each 2D material.

Experimentally, CuO/graphene was reported to have higher ISS than CuO/MoS_2, while this was found to be the case for CuO (Cu-surface) and Cu_2O+CuO (Cu-surface) for the simulations (Table 1 and Supporting Information; Table S2), suggesting that the experimental CuO samples had a more copper-rich surface.

In comparing counter-surfaces for the same 2D material (e.g. CuO/graphene vs TiO_2/graphene), the experiments found CuO systems to always have lower ISS than TiO_2 for the same 2D material. However, for graphene simulations, this was only the case for CuO (O-surface)/graphene. For MoS_2, only the Cu_2O+CuO (Cu-surface)/MoS_2 simulated system had lower ISS than TiO_2 MoS_2. This suggests that Cu_2O+CuO (Cu-surface) dominates the interaction experimentally as it fits three of the four experimental comparison trends and the one exception might be due to presence of some oxygen termination on the CuO as well as possibly defect sites and factors not captured in the simulations.

Interestingly comparison between graphene and MoS_2 also highlighted that the difference in their tribological behavior is considerably greater against an oxidized-copper counter-surface and attributed to the change in interfacial energy. The 13.7x difference in maximum energy change (ΔMax $Energy_{CuO/graphene}$ vs ΔMax $Energy_{CuO/MoS2}$) between graphene and MoS_2 resulted in 6.9x increase in pull-off force ($F_{POF, CuO/graphene}$ vs. $F_{POF, CuO/MoS2}$) and higher friction ($F_{F, CuO/graphene}$ vs. $F_{POF, CuO/MoS2}$) against oxidized-copper counter-surface (Table 1). This also suggests that interfacial adhesion is more sensitive to the change in surface energy corrugation than friction.

Against the oxidized-titanium counter-surface MoS_2 also exhibited lower friction and adhesion, however the difference (graphene vs MoS_2) is comparatively less substantial. Against oxidized-titanium counter-surface, there is only 1.9x difference in maximum energy change (ΔMax $Energy_{TiO2/graphene}$ vs ΔMax $Energy_{TiO2/MoS2}$) between graphene and MoS_2, resulting in 2.1x increase in pull-off force ($F_{POF, TiO2/graphene}$ vs. $F_{POF, TiO2/MoS2}$) and higher friction ($F_{F, TiO2/graphene}$ vs. $F_{F, TiO2/MoS2}$).

It should be noted that differences between ISS values for the simulations are far more pronounced than for experiments. The simulations utilize idealized surfaces and are mainly capturing the electronic effect of surface chemical species on the sliding behavior in static equilibrium snapshots. The dynamics of kinetic friction are not captured by the simulation. The experimental values are in effect measuring the average of various contributions to sliding force over an area orders of magnitude larger than the simulation cell. There will also be other factors such as contact size, surface morphology (fragments, holes, islands), defects, hetergenous layering, sliding oreintation, thermal effects, contaminants, environmental conditions (including humidity which was not zero for the experiments) and internal mechanical processes involving dissipiation of stress, internal layer movement or structural reconfiguration which may add to or contrast with these electronic effects in real-world applications and experiments and as such may be dwarfing the purely electronic effect differences captured by DFT simulations. The ISS experimental results thus suggest that chemical interacitons are not the dominant contributor to friction during interfacial shearing.

The metal oxides are less likely to be well described by atomic scale simulations than the 2D materials as the latter are actually atomically thin and have simpler structures. One of the experimental metal oxide surfaces might differ more from its DFT representation than the other. Therefore, comparing trends for the same metal oxide surface should be more reliable than across the two different metal surfaces and the former do follow the experimental trends exactly. For example, if the DFT TiO_2 surface ISS values were to rise while retaining their relative trend, all four experimental trends would match DFT. Perhaps the experimental TiO_2 surfaces are further away from the idealized surfaces, potentially due to increased defects and surface imperfections which are likely to raise ISS experimental values. However, we cannot isolate what are the other factors affecting the experiments which are not captured by DFT and this should be further investigated in future studies.

Conclusions

This study investigated the tribological behavior of metal counter-surfaces (i.e. titanium and copper) with 2D-materials (i.e. graphene and MoS_2). The metal surfaces underwent native oxidation with the formation of few nanometers thick TiO_2 and CuO layers. These oxides played an important role in the interfacial properties and exhibited chemical like interactions for most of the interfaces studied herein. Experimentally, higher friction force and adhesion were measured on graphene than on MoS_2 for both the metal-oxide counter-surfaces (i.e. TiO_2 and CuO).

In the case of TiO_2 counter-surface, DFT simulations also predicted lower friction on MoS_2. Comparison of monolayer vs bilayer MoS_2 showed no significant change in relative energy and ISS. This indicates that the thickness of 2D materials will have minimal influence on the chemical interaction of sliding metal-oxide counter-surfaces. In the case of CuO counter-surface, two possible exposed terminations were identified (O- vs Cu-surfaces), and both were found to influence the overall interaction in simulations (the two cannot be differentiated experimentally). For CuO (O-surface), sliding on graphene was found to have a lower ISS than MoS_2 while for CuO (Cu-surface) the opposite behavior was observed. This is suggestive that the Cu-surface dominates the interfacial interaction experimentally.

Experimental and DFT comparisons also identified the dependence between the tribological behavior, the interfacial electronic charge, and the changing interfacial energy profile along the metal-oxide/2D-materials interfaces. While the majority of interfaces are interacting chemically, the metal-oxide/2D-material interfaces exhibit varying interfacial behavior suggesting other dominating interfacial mechanisms. The small differences in ISS for the same meta-oxide countersurface experimentally in comparison to DFT results likely means that non chemcial interaction factors overwhelm electronic effects for shear behaviour. More homogenous interfacial charge distribution/sharing and lower surface energy variation, such as that observed for the TiO_2/MoS_2 and CuO (Cu-surface)/MoS_2 interfaces, were identified to lower friction and adhesion. The finding from this study is suggestive to combine MoS_2 with metal-oxide counter-surface if lower adhesion and easier shearing at the interface is preferred when

designing nanoscale oxidized-metals/2D-material hybrid systems. However, graphene should be preferred over MoS_2 if the metal-oxide counter-surface is highly oxygen terminated.

Methodology

Experimental

Sample Preparation, AFM Cantilever and Characterization. Graphene and MoS_2 samples were prepared by mechanical exfoliation using scotch tape method. Highly oriented pyrolytic graphite (SPI supplies) and a large MoS_2 crystal (Graphene supermarket) were used to peel and deposit ultrathin sheets onto n-doped silicon wafer substrate (Graphene supermarket). The surface of silicon substrate was clean using ethanol and methanol in an ultrasonic bath prior to exfoliation. AFM measurements show the thickness for 2D materials as 6.6 nm for MoS_2 and 4.2 nm for graphene. The custom fabricated AFM cantilevers were prepared by attaching copper and titanium (Alfa Aesar) beads of 99.9% and 99.5% purity onto tipless cantilevers (APP-Nano). A custom built microscope-micromanipulator setup was used to apply the PC-Super epoxy and attached the metal beads (bead radius of 2.5 μm for titanium and 3.5 μm for copper). The same beaded cantilevers were used to avoid the influence of bead shape or size when compare the 2D materials. A Hitachi scanning electron microscope (SU3500) was used for image the cantilevers. X-ray photoelectron spectroscopy (XPS) was performed using an ESCALAB 250Xi (Thermo Fisher Scientific - East Grinstead, UK) to identity and measure the thickness of oxide layers on the copper and titanium beads. The ESCALAB 250Xi system is equipped with monochromatic Al K_α X-ray source and was used to collect the survey spectra with pass energy (PE) of 100 eV and nominal spot size of 400 μm. Surface characerization was followed by the spectral regions of interest at higher resolution (PE - 20 eV) from which the composition (Rel. At.%) was obtained.

Tribology measurements. The Asylum Research MFP 3D atomic force microscope was used to perform friction force microscopy (FFM) and adhesion experiments. FFM and adhesion experiments were done using the custom fabricated copper and titanium cantilevers. The normal and torsion stiffness of the cantilevers were measuring using Sader's method. [35,36] The normal stiffness was measured ~5.4 N/m for copper and ~2.6 N/m for titanium cantilevers. Test probe method [37] was used to acquire the lateral sensitivity against a cleaved potassium bromide block and the normal sensitivity was measured by deflecting against silicon wafer. Friction voltage was measured as half the differences between the lateral trace and retrace signals as the cantilever slides at 90° scan angle with scan speed of ~5 μm/s. Using the FFM (friction vs. normal load) data, the experimental interfacial shear strength (ISS) was calculated by fitting the generalized Maugis–Dugdale model proposed by Carpick et al.[31] The fitting of the generalized Maugis–Dugdale model allows for the extraction of pull off forces and , where indicates the transition between JKR and DMT models (corresponds to the JKR case and corresponds to the DMT case). Using these extracted parameters, the transition parameter ( ) and interfacial energy ( ) can be determined, allowing for the estimation of the contact radius (and calculating ISS experimentally. Detailed ISS fitting procedure is provided in the supporting information (Supporting Information; Section

S2). Lastly, adhesion experiments were done with maximum normal load of 90nN and dwell time of 1s. Dry environment was acquired by purging the environment locally around the contact with 99.9% pure N_2 gas.

Simulations

Plane wave-based DFT was run through the Quantum Espresso software package.[38,39] Interactions between the valence electrons and the ionic core were represented by the projector augmented wave (PAW) [40] method with Perdew–Burke–Ernzerhof (PBE) formulation. Kinetic energy cutoffs of 748 eV (55 Ry) and 8163 eV (600 Ry) were used for the wave functions and the charge density, respectively. All calculations were non spin polarized and van der Waals corrections were applied through Grimme's DFT-D3 method with Becke-Jonson (BJ) damping.[41,42] A Monkhorst-Pack defined mesh of 2 x 2 x 1 k-points was used to sample the Brillouin zone. Adsorption distance was based on taking average position of surface atoms for each surface of the interface and then finding the difference in these two average positions.

All material systems were modelled periodically, where the surfaces were brought to a separation of 2.3 Å and the interface was allowed to relax in the out-of-plane direction (normal to each surface) for the most stable interfacial separation distance. The (001) plane of each metal oxide surface (CuO & TiO_2) was tested against both graphene and MoS_2. For the oxidized metal counter-surfaces, only the layers closest to the interface were allowed to relax while those further away were fixed in order to simulate the bulk solid. The 2D sheet was then moved in the in-plane direction by a 0.33 Å step displacement (Δd) and again relaxed in the out-of-plane direction for a total of 10 steps. This simulates a pseudo-sliding motion where the surfaces are allowed to reach equlibrium separation distances at discrete points along the sliding path. Note that this does not simulate a dynamic process such as found in kinetic friction measurements or those with applied loads (no load is applied in the simulations and the systems are relaxed at absolute zero in a vaccum).

Declarations

Funding (information that explains whether and by whom the research was supported)

- Hart Professorship
- Natural Sciences and Engineering Research Council of Canada

Conflicts of interest/Competing interests (include appropriate disclosures)

None

Availability of data and material (data transparency)

None

Code availability (software application or custom code)

Not applicable

Reference

1. Grandin, M.; Wiklund, U. Wear Phenomena and Tribofilm Formation of Copper/Copper-Graphite Sliding Electrical Contact Materials. *Wear* **2018**, *398–399* (December 2017), 227–235.
2. Mu, M.; Liang, J.; Zhou, X.; Xiao, Q. One-Step Preparation of TiO2/MoS2 Composite Coating on Ti6Al4V Alloy by Plasma Electrolytic Oxidation and Its Tribological Properties. *Surf. Coatings Technol.* **2013**, *214*, 124–130.
3. Li, J. F.; Zhang, L.; Xiao, J. K.; Zhou, K. C. Sliding Wear Behavior of Copper-Based Composites Reinforced with Graphene Nanosheets and Graphite. *Trans. Nonferrous Met. Soc. China (English Ed.* **2015**, *25* (10), 3354–3362.
4. Xu, Z. Y.; Xu, Y.; Hu, K. H.; Xu, Y. F.; Hu, X. G. Formation and Tribological Properties of Hollow Sphere-like Nano-MoS2 Precipitated in TiO2 Particles. *Tribol. Int.* **2015**, *81*, 139–148.
5. Alghani, W.; Ab Karim, M. S.; Bagheri, S.; Amran, N. A. M.; Gulzar, M. Enhancing the Tribological Behavior of Lubricating Oil by Adding TiO2, Graphene, and TiO2/Graphene Nanoparticles. *Tribol. Trans.* **2019**, *62* (3), 452–463.
6. Luo, J.; Jiang, S.; Zhang, H.; Jiang, J.; Liu, X. A Novel Non-Enzymatic Glucose Sensor Based on Cu Nanoparticle Modified Graphene Sheets Electrode. *Anal. Chim. Acta* **2012**, *709*, 47–53.
7. Xin, X.; Zhou, X.; Wu, J.; Yao, X.; Liu, Z. Scalable Synthesis of TiO2/Graphene Nanostructured Composite with High-Rate Performance for Lithium Ion Batteries. *ACS Nano* **2012**, *6* (12), 11035–11043.
8. Carrillo, I.; Rangel, E.; Magaña, L. F. Adsorption of Carbon Dioxide and Methane on Graphene with a High Titanium Coverage. *Carbon N. Y.* **2009**, *47* (11), 2758–2760.
9. Mai, Y. J.; Wang, X. L.; Xiang, J. Y.; Qiao, Y. Q.; Zhang, D.; Gu, C. D.; Tu, J. P. CuO/Graphene Composite as Anode Materials for Lithium-Ion Batteries. *Electrochim. Acta* **2011**, *56* (5), 2306–2311.
10. Chen, F.; Ying, J.; Wang, Y.; Du, S.; Liu, Z.; Huang, Q. Effects of Graphene Content on the Microstructure and Properties of Copper Matrix Composites. *Carbon N. Y.* **2016**, *96*, 836–842.
11. Chmielewski, M.; Michalczewski, R.; Piekoszewski, W.; Kalbarczyk, M. Tribological Behaviour of Copper-Graphene Composite Materials. *Key Eng. Mater.* **2016**, *674*, 219–224.
12. Grandin, M.; Wiklund, U. Influence of Mechanical and Electrical Load on a Copper/Copper-Graphite Sliding Electrical Contact. *Tribol. Int.* **2018**, *121* (September 2017), 1–9.
13. Fonseca, A. F.; Liang, T.; Zhang, D.; Choudhary, K.; Phillpot, S. R.; Sinnott, S. B. Graphene-Titanium Interfaces from Molecular Dynamics Simulations. *ACS Appl. Mater. Interfaces* **2017**, *9* (38), 33288–33297.

14. Dong, H. S.; Qi, S. J. Realising the Potential of Graphene-Based Materials for Biosurfaces – A Future Perspective. *Biosurface and Biotribology* **2015**, *1* (4), 229–248.
15. Xue, B.; Liu, X.; Shi, X.; Huang, Y.; Lu, G.; Wu, C. Effect of Graphene Nanoplatelets on Tribological Properties of Titanium Alloy Matrix Composites at Varying Sliding Velocities. *Mater. Res. Express* **2018**, *5* (6).
16. Hwang, B.; Kim, W.; Kim, J.; Lee, S.; Lim, S.; Kim, S.; Oh, S. H.; Ryu, S.; Han, S. M. Role of Graphene in Reducing Fatigue Damage in Cu/Gr Nanolayered Composite. *Nano Lett.* **2017**, *17* (8), 4740–4745.
17. Kim, Y.; Lee, J.; Yeom, M. S.; Shin, J. W.; Kim, H.; Cui, Y.; Kysar, J. W.; Hone, J.; Jung, Y.; Jeon, S.; et al. Strengthening Effect of Single-Atomic-Layer Graphene in Metal-Graphene Nanolayered Composites. *Nat. Commun.* **2013**, *4*, 1–7.
18. Adamska, L.; Lin, Y.; Ross, A. J.; Batzill, M.; Oleynik, I. I. Atomic and Electronic Structure of Simple Metal/Graphene and Complex Metal/Graphene/Metal Interfaces. *Phys. Rev. B - Condens. Matter Mater. Phys.* **2012**, *85* (19), 1–8.
19. Olsen, T.; Thygesen, K. S. Random Phase Approximation Applied to Solids, Molecules, and Graphene-Metal Interfaces: From van Der Waals to Covalent Bonding. *Phys. Rev. B - Condens. Matter Mater. Phys.* **2013**, *87* (7).
20. Kim, Y.; Lee, J.; Yeom, M. S.; Shin, J. W.; Kim, H.; Cui, Y.; Kysar, J. W.; Hone, J.; Jung, Y.; Jeon, S.; et al. Strengthening Effect of Single-Atomic-Layer Graphene in Metal-Graphene Nanolayered Composites. *Nat. Commun.* **2013**, *4*, 1–7.
21. Bagchi, S.; Ke, C.; Chew, H. B. Oxidation Effect on the Shear Strength of Graphene on Aluminum and Titanium Surfaces. *Phys. Rev. B* **2018**, *98* (17), 1–9.
22. Dai, Y.; Wu, X.; Du, C.; Deng, J.; Hu, L.; Hu, X. Density Functional Calculation of Transition Metal Adatom Adsorption on Graphene. *Phys. B Condens. Matter* **2010**, *405* (16), 3337–3341.
23. Khomyakov, P. A.; Giovannetti, G.; Rusu, P. C.; Brocks, G.; Van Den Brink, J.; Kelly, P. J. First-Principles Study of the Interaction and Charge Transfer between Graphene and Metals. *Phys. Rev. B - Condens. Matter Mater. Phys.* **2009**, *79* (19), 1–12.
24. Williams, G.; Seger, B.; Kamat, P. V. UV-Assisted Photocatalytic Reduction of Graphene Oxide. **2008**, *2* (7), 1487–1491.
25. Wolloch, M.; Feldbauer, G.; Mohn, P.; Redinger, J.; Vernes, A. Ab Initio Friction Forces on the Nanoscale: A Density Functional Theory Study of Fcc Cu(111). *Phys. Rev. B - Condens. Matter Mater. Phys.* **2014**, *90* (19), 1–8.
26. Wolloch, M.; Levita, G.; Restuccia, P.; Righi, M. C. Interfacial Charge Density and Its Connection to Adhesion and Frictional Forces. *Phys. Rev. Lett.* **2018**, *121* (2), 26804.
27. Arif, T.; Yadav, S.; Colas, G.; Singh, C. V.; Filleter, T. Understanding the Independent and Interdependent Role of Water and Oxidation on the Tribology of Ultrathin Molybdenum Disulfide (MoS2). *Adv. Mater. Interfaces* **2019**, *1901246*, 1–9.
28. Scanlon, D. O.; Dunnill, C. W.; Buckeridge, J.; Shevlin, S. A.; Logsdail, A. J.; Woodley, S. M.; Catlow, C. R. A.; Powell, M. J.; Palgrave, R. G.; Parkin, I. P.; et al. Band Alignment of Rutile and Anatase TiO2. *Nat.*

Mater. **2013**, *12* (9), 798–801.

29. Keil, P.; Lützenkirchen-Hecht, D.; Frahm, R. Investigation of Room Temperature Oxidation of Cu in Air by Yoneda-XAFS. *AIP Conf. Proc.* **2007**, *882*, 490–492.
30. Keil, P.; Frahm, R.; Lützenkirchen-Hecht, D. Native Oxidation of Sputter Deposited Polycrystalline Copper Thin Films during Short and Long Exposure Times: Comparative Investigation by Specular and Non-Specular Grazing Incidence X-Ray Absorption Spectroscopy. *Corros. Sci.* **2010**, *52* (4), 1305–1316.
31. Carpick, R. W.; Ogletree, D. F.; Salmeron, M. A General Equation for Fitting Contact Area and Friction vs Load Measurements. *J. Colloid Interface Sci.* **1999**, *211* (2), 395–400.
32. Vazirisereshk, M. R.; Ye, H.; Ye, Z.; Otero-de-la-Roza, A.; Zhao, M.-Q.; Gao, Z.; Johnson, A. T. C.; Johnson, E. R.; Carpick, R. W.; Martini, A. Origin of Nanoscale Friction Contrast between Supported Graphene, MoS2 , and a Graphene/MoS2 Heterostructure. *Nano Lett.* **2019**, *19* (8), 5496–5505.
33. Dong, H.; Xu, Y.; Zhang, C.; Wu, Y.; Zhou, M.; Liu, L.; Dong, Y.; Fu, Q.; Wu, M.; Lei, Y. MoS2 Nanosheets with Expanded Interlayer Spacing for Enhanced Sodium Storage. *Inorg. Chem. Front.* **2018**, *5* (12), 3099–3105.
34. Çakmak, G.; Öztürk, T. Continuous Synthesis of Graphite with Tunable Interlayer Distance. *Diam. Relat. Mater.* **2019**, *96*, 134–139.
35. Sader, J. E.; Chon, J. W. M.; Mulvaney, P. Calibration of Rectangular Atomic Force Microscope Cantilevers. *Rev. Sci. Instrum.* **1999**, *70* (10), 3967–3969.
36. Green, C. P.; Lioe, H.; Cleveland, J. P.; Proksch, R.; Mulvaney, P.; Sader, J. E. Normal and Torsional Spring Constants of Atomic Force Microscope Cantilevers. *Rev. Sci. Instrum.* **2004**, *75* (6), 1988–1996.
37. Cannara, R. J.; Eglin, M.; Carpick, R. W. Lateral Force Calibration in Atomic Force Microscopy: A New Lateral Force Calibration Method and General Guidelines for Optimization. *Rev. Sci. Instrum.* **2006**, *77* (5), 053701.
38. Giannozzi, P.; Andreussi, O.; Brumme, T.; Bunau, O.; Buongiorno Nardelli, M.; Calandra, M.; Car, R.; Cavazzoni, C.; Ceresoli, D.; Cococcioni, M.; et al. Advanced Capabilities for Materials Modelling with Quantum ESPRESSO. *J. Phys. Condens. Matter* **2017**.
39. Giannozzi, P.; Baroni, S.; Bonini, N.; Calandra, M.; Car, R.; Cavazzoni, C.; Ceresoli, D.; Chiarotti, G. L.; Cococcioni, M.; Dabo, I.; et al. QUANTUM ESPRESSO: A Modular and Open-Source Software Project for Quantum Simulations of Materials. *J. Phys. Condens. Matter* **2009**.
40. Kresse, G.; Joubert, D. Kresse, Joubert - Unknown - From Ultrasoft Pseudopotentials to the Projector Augmented-Wave Method. *Phys. Rev. B* **1999**, *59* (3), 11–19.
41. Grimme, S.; Ehrlich, S.; Goerigk, L. Effect of the Damping Function in Dispersion Corrected Density Functional Theory. *J. Comput. Chem.* **2011**.
42. Grimme, S.; Antony, J.; Ehrlich, S.; Krieg, H. A Consistent and Accurate Ab Initio Parametrization of Density Functional Dispersion Correction (DFT-D) for the 94 Elements H-Pu. *J. Chem. Phys.* **2010**.

Figures

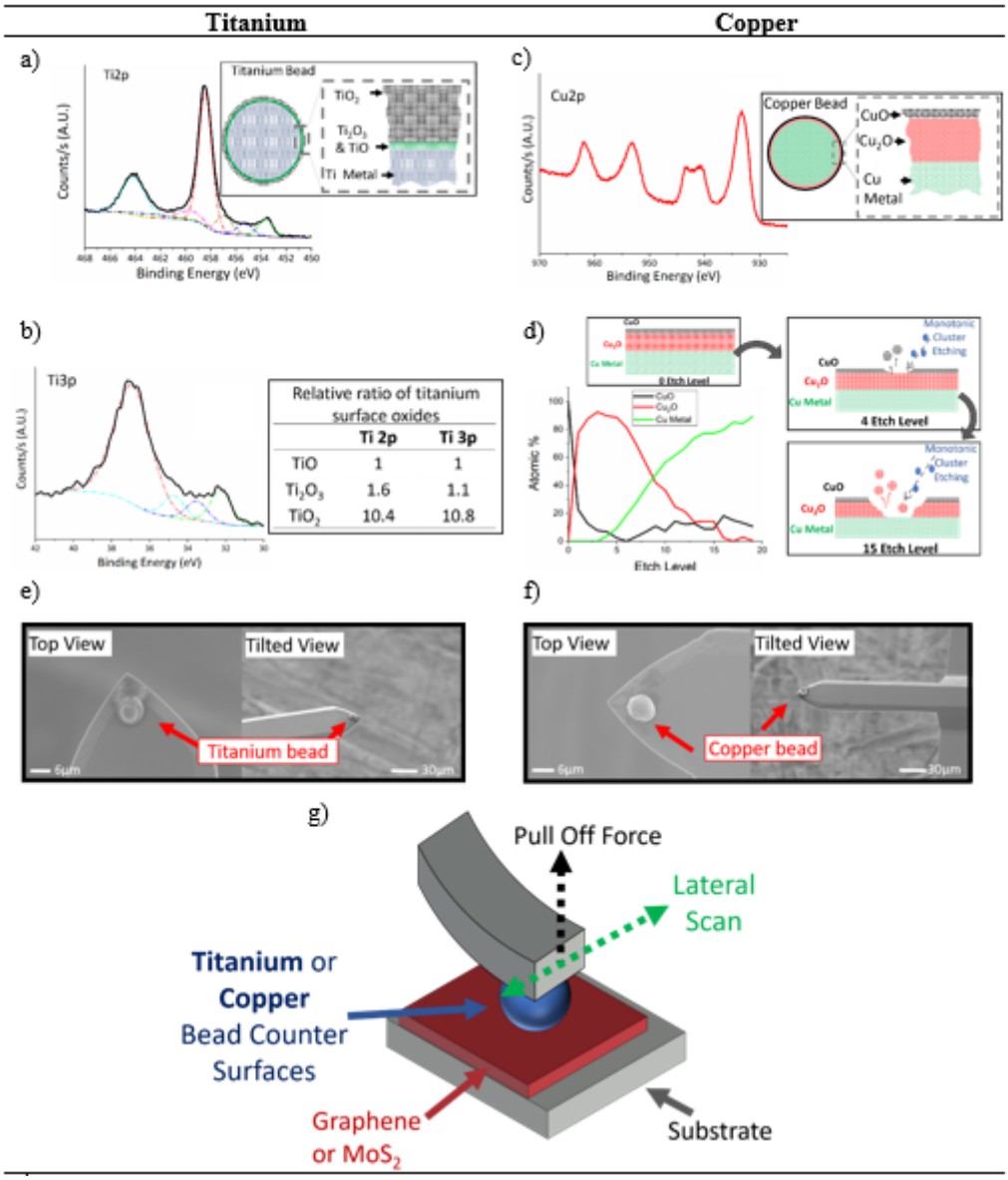

Figure 1

a) High resolution XPS of titanium powder Ti2p. Inset: Schematic of titanium bead surface chemistry. b) High resolution XPS of titanium powder Ti3p. Inset: Relative ratio of titanium oxides normalized to TiO obtained from fitting Ti2p and Ti3p peaks. c) High resolution XPS of copper powder at Cu2p. Inset: Schematic of copper bead surface chemistry. d) Atomic% as a function of etched depth using the copper auger peak for surface chemistry depth profile on copper powder. Insets: Schematic for etch levels 0, 4 and 15. Top (2000x) and tilted (500x) SEM images of e) titanium and f) copper beaded AFM cantilevers. g) Schematic of the experimental setup and the interfaces studied.

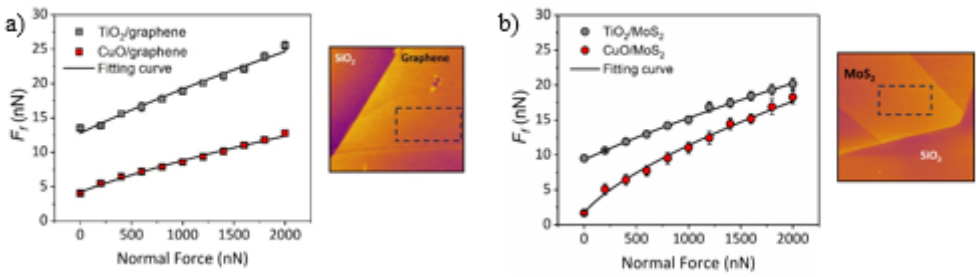

Figure 2

a) Comparison of average friction force as a function of normal load on graphene samples using CuO and TiO2 counter-surfaces in room condition (RH18%). Right inset: Graphene topography image (10x10 μm). b) Comparison of average friction force as a function of normal load on MoS2 samples using CuO and TiO2 counter-surfaces in room condition (RH18%). Right inset: MoS2 topography image (8x8 μm). Friction force data fitted using the generalized Maugis–Dugdale fitting model for measuring interfacial shear strength (ISS).31

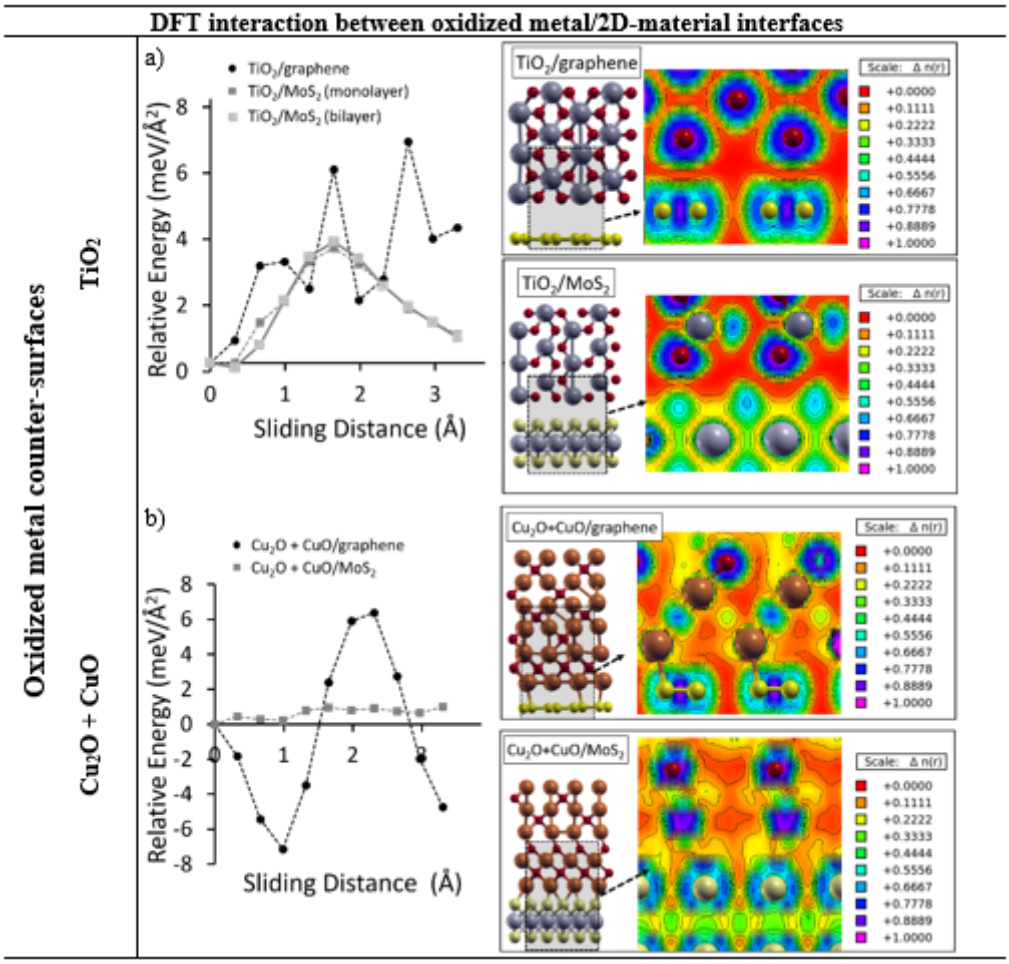

Figure 3

a) DFT-based interaction of TiO2/2D-materials (graphene and MoS2) for tracking the relative energy change during sliding. Insets: DFT material system and ELF analysis for TiO2/2D-material interfaces. b) DFT-based interaction of Cu2O+CuO/2D-materials (graphene and MoS2) for tracking the relative energy change during sliding. Insets: DFT material system and ELF analysis for Cu2O+CuO/2D-material interfaces. Purple grey atoms are Mo or Ti, red atoms are O, bright yellow atoms are C and pale yellow atoms are S.

Supplementary Files

This is a list of supplementary files associated with this preprint. Click to download.

- Manuscript4V16SI.docx